

ELECTRONIC SUPPLEMENTARY INFORMATION (ESI)

Surface specificity and mechanistic pathway of de-fluorination of C₆₀F₄₈ on coinage metals

Rogger Palacios-Rivera,¹ David C. Malaspina,¹ Nir Tessler,² Olga Solomeshch,² Jordi Faraudo,^{1} Esther Barrena^{1*} and Carmen Ocal¹*

¹Institut de Ciència de Materials de Barcelona (ICMAB-CSIC), Campus UAB, Bellaterra, E-08193, Barcelona, Spain

²Electrical Engineering Department, Nanoelectronic Center, Technion, Haifa 32000, Israel

In addition to the present Supplementary Information, we also provide two videos with MD simulations describing: a) the molecular adsorption process, where de-fluorination of C₆₀F₄₈ when approaching a Ni(111) surface is visualized and b) the molecular rotation process, showing the change in position (translation plus rotation) of one molecule on the surface.

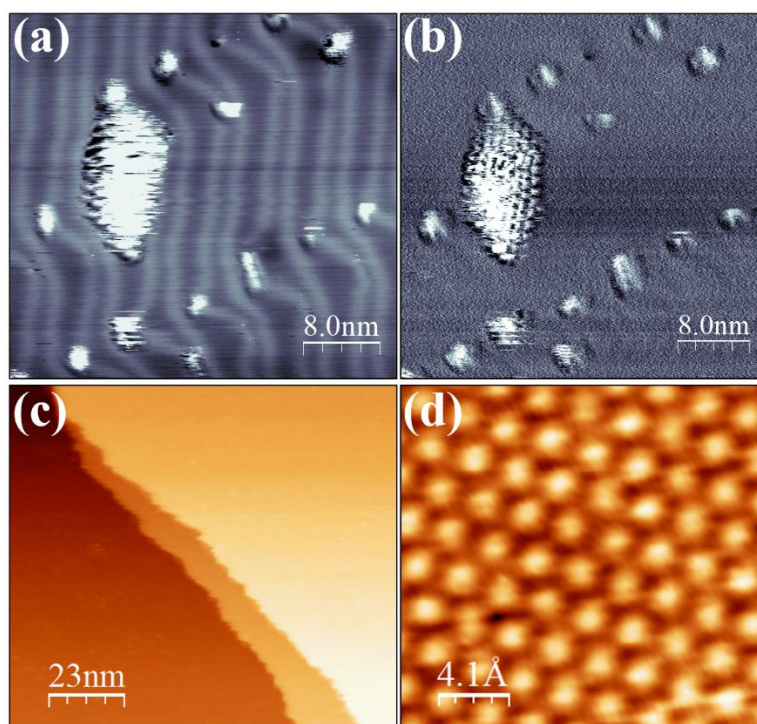


Figure S1. STM images of low deposits of $C_{60}F_{48}$ molecules on Au(111) surface using the constant current mode. Simultaneously measured (a) topographic and (b) frequency shift (Δf) channels. The two images clearly show monomers and dimers nucleated at the pinched elbows of the herringbone (HB) reconstruction of Au(111). Their frizzy aspect is due to molecular motion within the trapping points. Note the hexagonal packing visible in Δf . The STM was calibrated by using atomic resolution images of clean single crystals as Cu(111) or Au(111). Here we show large scale (c) and atomic scale (d) STM images of Cu(111) used for Z and X, Y piezo calibration, respectively, via monoatomic step height and surface unit cell. STM parameters: (a-b) $I = 200$ pA, bias = +1.8 V. (c) $I = 376$ pA, bias = -1.4 V. and (d) $I = 240$ pA, bias = -0.32 V.

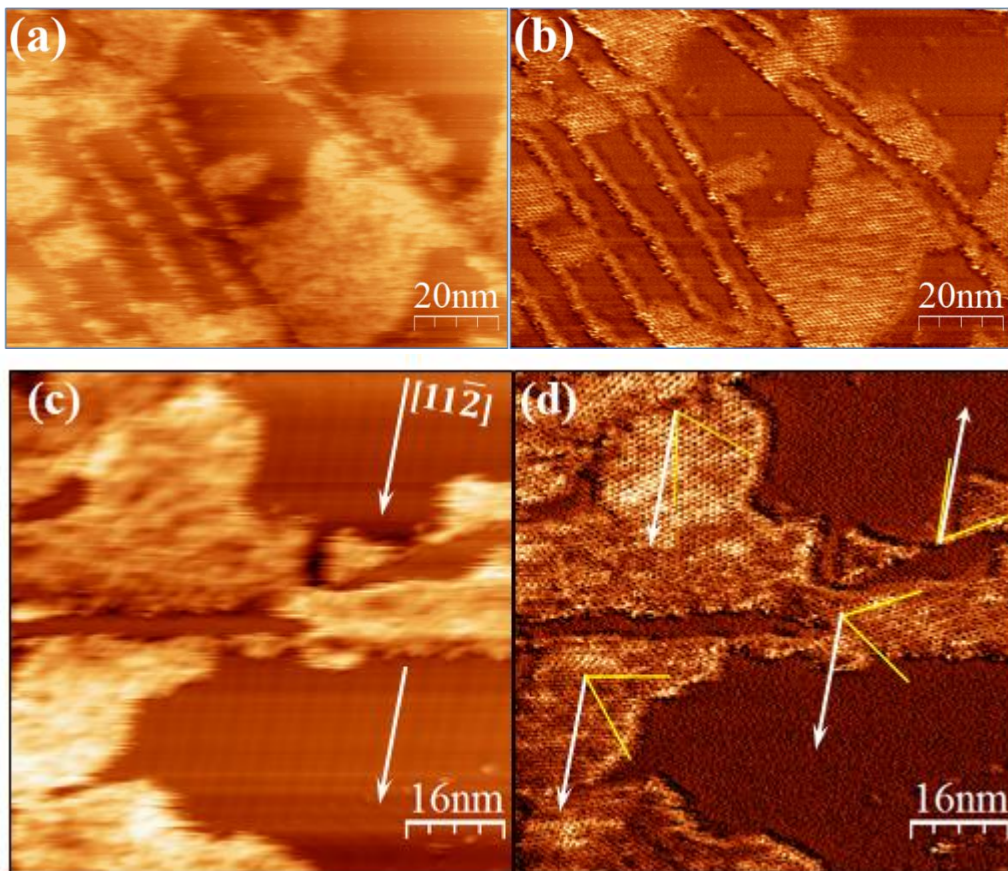


Figure S2. STM images of about half monolayer of $C_{60}F_{48}$ molecules on Au(111) surface using the constant current mode. (a, c) Topographic and simultaneously measured (b, d) frequency shift (Δf) channels. In the upper panels, the $C_{60}F_{48}$ molecules decorate the step edges and form islands that extend over the terraces. In the lower panels, islands on the same terrace show diverse orientations (indicated by yellow lines in d) misaligned with respect to the substrate. White arrows in all images correspond to the $[11\bar{2}]$ direction and can be used as in-situ reference for domain orientation. Note that a unique and undistorted HB domain exists in the whole image (c) under the islands, pointing to a weak adsorbate-substrate interaction. As commented in the manuscript, despite the blurring appearance of the $C_{60}F_{48}$ islands in topography (a, c), the Δf image clearly shows the hexagonal order of the molecular packing. STM parameters: (a, b) $I = 190$ pA, bias = + 3.0 V; (c, d) $I = 200$ pA, bias = +1.8 V.

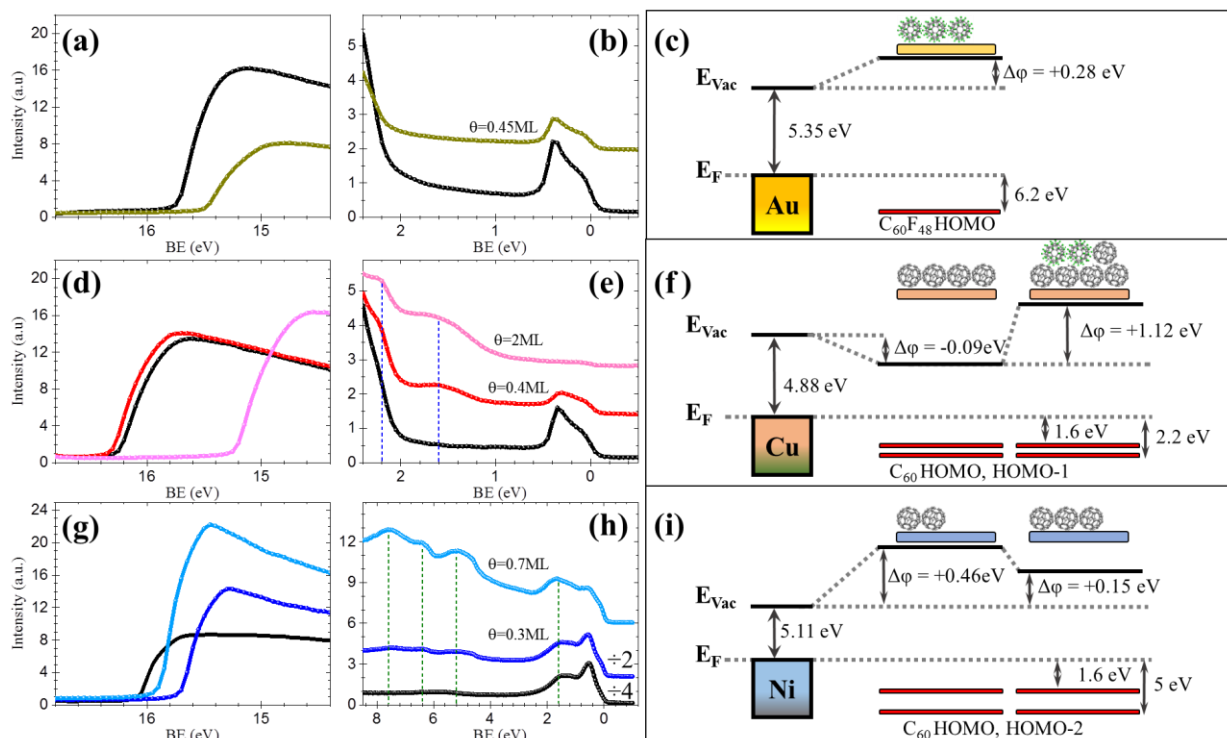


Figure S3. Secondary electron cutoff (SECO) and near Fermi-edge valence band (VB) density of states as measured by UPS, for different coverages of $C_{60}F_{48}$ on: (a, b) Au(111), (d, e) Cu(111) and (g, h) Ni(111). Black data in all panels correspond to the spectra for the respective bare metals. The diverse $C_{60}F_{48}$ coverages are: $\theta=0.45$ ML green data in (a, b), $\theta=0.4$ ML and $\theta=2$ ML as red and pink in (d, e) and $\theta=0.3$ ML and $\theta=0.7$ ML dark blue and light blue in (g, h). The shifts in vacuum level (E_{vac}) extracted from SECO and the highest occupied molecular orbital (HOMOs) positions are represented in (c), (f) and (i) in the energy levels diagram for each case. **BV description:** (b) In consistency with the deep-lying HOMO level of $C_{60}F_{48}$, there is no extra feature close to the fermi level with respect of that of the clean Au(111). (e) For low $C_{60}F_{48}$ coverage on Cu(111), two HOMO levels at ≈ 1.8 eV and ≈ 2.2 eV are characteristic frontier orbitals of the C_{60} on Cu(111), indicating de-fluorination. (h) for Ni(111), the HOMO of C_{60} can be appreciated at ≈ 1.7 eV along with clear observation of deeper occupied molecular orbitals (up to HOMO-5) in excellent agreement with those of C_{60} on Ni substrates, i.e., indicating as well de-fluorination of the impinging molecules.

Fluorine content on the surface: XPS core level analysis

In order to perform quantitative analysis of the measured intensity (I) in the XPS spectra, we first estimate the relative cross section for the measured C1s and F1s core levels taking into account that the intensity (area) of each peak is proportional to the number of atoms within this energetic surrounding, for example:

$$I(\text{C-C}) = \sigma(\text{C1s}) \cdot n(\text{C-C})$$

Where $n(\text{C-C})$ is the total number of C atoms bonded only to other C atoms and $\sigma(\text{C1s})$ the corresponding cross section at the C1s binding energy region. Because independently of the fluorine content $n(\text{C-F}) = n(\text{F-C})$, the ratio between the intensity (area) of the corresponding peaks, $I(\text{C-F})/I(\text{F-C})$ is equal to the inverse relative cross section between F1s and C1s core levels $R = \sigma(\text{F}) / \sigma(\text{C})$:

$$n(\text{F-C})/n(\text{C-F}) = \sigma(\text{C}) / \sigma(\text{F}) \cdot I(\text{F-C}) / I(\text{C-F}) = [1/ R] \cdot [I(\text{F-C}) / I(\text{C-F})] = 1$$

By using the XPS data for the deposition on Au(111) we obtain $R = 5$

Secondly, whatever it is the degree of $\text{C}_{60}\text{F}_{48}$ de-fluorination in the metal surface, the total number of molecules at the surface (unperturbed plus de-fluorinated molecules) can be extracted from the total intensity of all components of the C1s peak:

$$n(\text{C}) \propto I(\text{C-C}) + I(\text{C-CF}) + I(\text{C-F})$$

$$n(\text{F}) \propto I(\text{F-C}) + I(\text{F-metal})$$

Where $n(\text{C})$ is the total number of C atoms, $I(\text{C-C})$ correspond to full de-fluorinated fullerenes (C_{60}), $I(\text{C-CF})$ and $I(\text{C-F})$ correspond to C bonded only to C atoms and to F atoms in molecules retaining F, respectively. On the other hand, $I(\text{F-C})$ and $I(\text{F-metal})$ stand for the fluorine bonded to C and to the metal surface, respectively. The ascription of all peaks is detailed by their BE in the main manuscript. Thus, for each deposited molecule, the percentage of fluorine atoms (F_s) that remain on each metal surface can be estimated from the ratio between the number of F bonded to the corresponding metal and the total number of carbon atoms, $n(\text{C})$.

$$F_s(\text{metal}) = [1/R] \cdot [I(\text{F-metal}) / \{I(\text{C-C}) + I(\text{C-CF}) + I(\text{C-F})\}]$$

For the intensity of the different peaks, we consider the area (A) obtained from the corresponding XPS data fits (Figure S4). For de-fluorination of C₆₀F₄₈ on Cu(111) and Ni(111) at the coverages studied in the present work (Figure 3 in the main manuscript), the results are:

$\theta = 0.4 \text{ ML on Cu(111)}$: $F_s(\text{Cu}) = 0$ No F-metal peak is detected on the surface (**0%**)

$\theta = 2 \text{ ML on Cu(111)}$: $F_s(\text{Cu}) = [1/R] \cdot [A(\text{F-Cu}) / \{A(\text{C-C}) + A(\text{C-CF}) + A(\text{C-F})\}] = 0.35$ (**35%**)

$\theta = 0.3 \text{ ML on Ni(111)}$: $F_s(\text{Cu}) = [1/R] \cdot [A(\text{F-Ni}) / \{A(\text{C-C})\}] = 0.10$ (**10%**)

$\theta = 0.7 \text{ ML on Ni(111)}$: $F_s(\text{Ni}) = [1/R] \cdot [A(\text{F-Ni}) / A(\text{C-C})] = 0.43$ (**43%**)

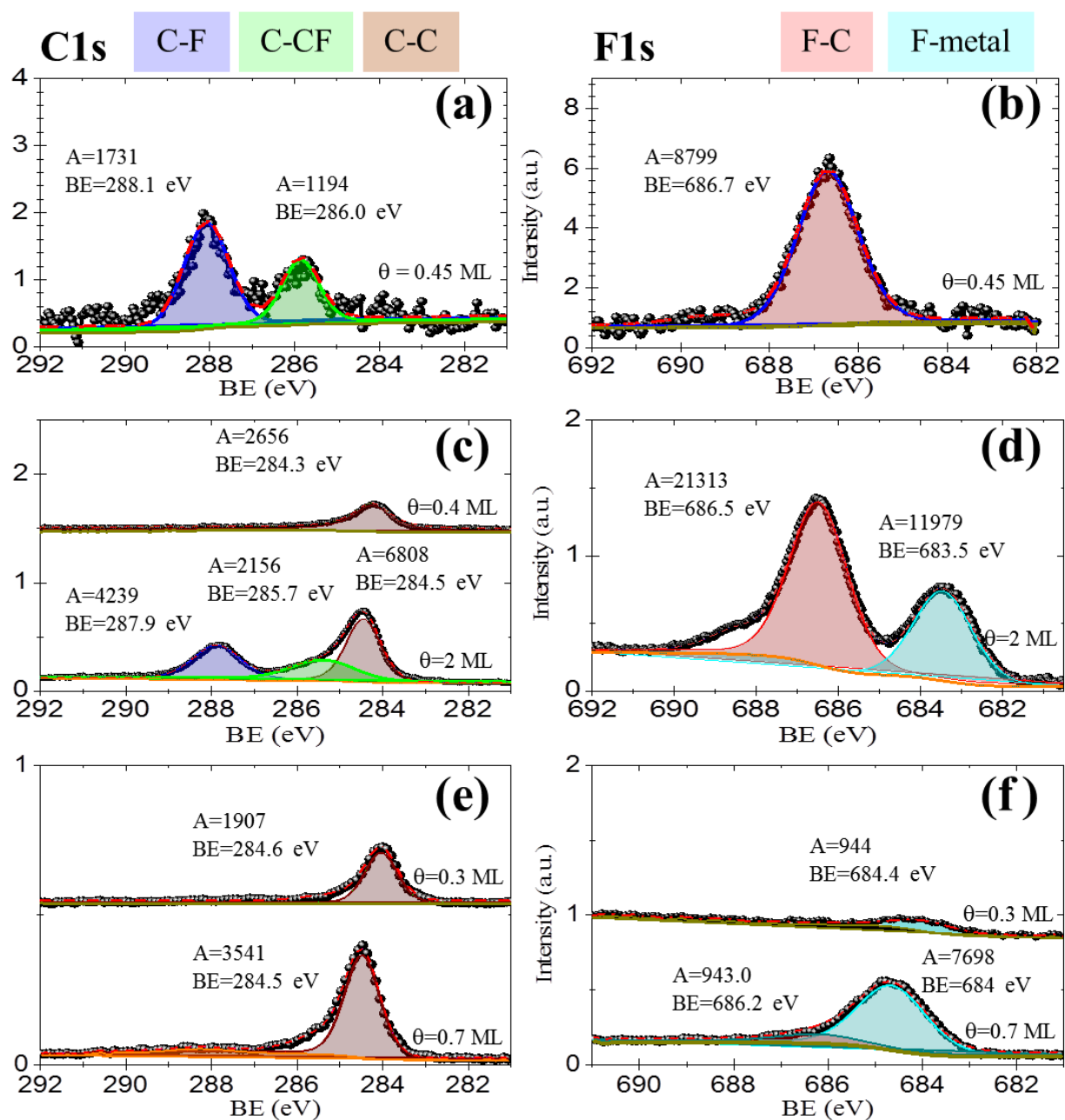


Figure S4. XPS spectra of the C1s and F1s core levels for diverse deposition of $C_{60}F_{48}$ on: (a,b) Au(111), (c,d) Cu(111) and (e,f) Ni(111). The coverage (θ) is given for each case. The areas (A) are given in arbitrary units calculated from the corresponding fits (coloured regions) at the indicated binding energy (BE). The peaks labels (C-F, C-CF, C-C, F-C and F-metal) are those as ascribed in the main manuscript.

Molecular Dynamics: technical details

The protocol for our MD simulations of $C_{60}F_{48}$ onto a Ni(111) surface was the following. The initial coordinates for $C_{60}F_{48}$ were built by adding fluorine atoms to a C_{60} obtained from the crystallographic structure with code PDB:5HKR.¹ The one by one addition of F atoms was performed following the pathway proposed from a previous DFT study of fluorination of fullerene.² The resulting structure was further equilibrated and thermalized by running a short MD simulation at 300K. The atomic coordinates for the metal surface were obtained by replicating the unit cell of Ni in the crystallographic plane (1,1,1) thermalized and equilibrated by running a short MD simulation at 300K and 1 atm of pressure. The resulting Ni(111) structure was made by 840 atoms arranged in 5 atomic layers with an area of 9.6 nm^2 . These coordinates of both $C_{60}F_{48}$ and Ni were combined by initially placing a $C_{60}F_{48}$ molecule at a distance of $\sim 6 \text{ \AA}$ from the Ni(111) (measured as the distance between the nearest C and Ni atoms). Periodic boundary conditions were employed in all directions, with a large simulation box of size $31.08 \times 30.89 \times 180.0 \text{ \AA}^3$. Initially, the system was prepared out of equilibrium by considering the molecules in the gas phase hotter than the surface, as in the experimental cell (this also makes the motion of $C_{60}F_{48}$ in the gas phase faster, speeding up these otherwise very slow simulations). We assigned an initial temperature of $\sim 500 \text{ K}$ to the $C_{60}F_{48}$ molecule. The thermostat at 300K was coupled to the Ni atoms during all the simulation. The simulated MD trajectory was processed combining the Visual Molecular Dynamics (VMD) software for the snapshot analysis and movies³ and custom scripts for data analysis.

See provided movies.

References

- (1) Kim, K.-H.; Ko, D.-K.; Kim, Y.-T.; Kim, N. H.; Paul, J.; Zhang, S.-Q.; Murray, C. B.; Acharya, R.; DeGrado, W. F.; Kim, Y. H.; et al. Protein-Directed Self-Assembly of a Fullerene Crystal. *Nat. Commun.* **2016**, *7* (1), 11429.
<https://doi.org/10.1038/ncomms11429>
- (2) Sheka, E. F. Stepwise Computational Synthesis of Fullerene C60 Derivatives. Fluorinated Fullerenes C60F2k. *J. Exp. Theor. Phys.* **2010**, *111* (3), 397–414.
<https://doi.org/10.1134/S1063776110090098>
- (3) Humphrey, W.; Dalke, A.; Schulten, K. VMD: Visual Molecular Dynamics. *J. Mol. Graph.* **1996**, *14* (1), 33–38. [https://doi.org/10.1016/0263-7855\(96\)00018-5](https://doi.org/10.1016/0263-7855(96)00018-5)